Polymer 51 (2010) 1176–1190

Contents lists available at ScienceDirect

Polymer

journal homepage: www.elsevier.com/locate/polymer

Understanding interfacial polycondensation: Experiments on polyurea system and comparison with theory

Sunil S. Dhumal, A.K. Suresh*

Department of Chemical Engineering, Indian Institute of Technology, Bombay 400076, India

ARTICLE INFO

Article history:
Received 30 September 2009
Received in revised form
27 December 2009
Accepted 5 January 2010
Available online 13 January 2010

Keywords:
Interfacial polycondensation
Polyurea
Molecular weight distribution

ABSTRACT

Interfacial polycondensation, with its multiphase character and the involvement of several rate and equilibrium processes, presents unique challenges to our ability to understand and design processes for achieving desired properties. In a recent study [1], we have presented a detailed model for the process and shown that it explains the salient features as reported in the literature for several interfacial systems. In the present paper, we report extensive experimental studies on the polyurea system and their comparison with the model. Two geometries – the spherical geometry of the microcapsule and the flat-film geometry – have been used to study qualitative and quantitative features of the polycondensation and the nature of the film that forms. While some aspects, such as the manner in which the solvent influences the kinetics, confirm earlier findings, inadequacies have been identified in the sample preparation protocols followed in earlier work, because of which property estimations may carry a large error. Improved protocols have accordingly been developed and used to study the development of film properties in time and as a function of the important preparation variables. Detailed molecular weight distributions have been determined using a GPC technique and used to derive important properties of the polyurea (such as Mark–Houwink parameters) as well as to gain insights into mechanisms. The data have been used to determine the rate parameters in the Dhumal and Suresh [1] model. The predictions of the model, as far as trends are concerned, are shown to be satisfactory given the level of uncertainty about parameter values and the complexity of the system being studied. Where discrepancies exist, the reasons have been established and the areas for improvement of the model identified. The findings reported are of interest to applications such as controlled release and membrane separations, in which permeation rate through the membrane is of importance and depends upon various membrane properties like crystallinity, morphology, etc.

1. Introduction

Since the time of its discovery, the interfacial polycondensation (IP) technique has seen a wide range of applications, such as synthesis of bulk polymers [2,3], micro/nano-capsules [4–8], thin film composite/nanocomposite membranes (TFCM) [9–15], polymer nanocomposites [16,17], surface modification of fibers [18,19], micro-unit operations [20,21] and self healing materials [22]. This has motivated the research community to study extensively both experimental and theoretical aspects of the IP process. In general, IP offers the possibility of rapid production of polymers (linear or cross linked) with high and specific molecular weight ranges under normal conditions of temperature and pressure at/or near the interface of two immiscible phases, either liquid–liquid or gas liquid. The performance of the formed polymer coat, film or membrane, depends upon the chemical composition of the polymer as well as properties such as film thickness, crystallinity, molecular weight, degree of cross linking, mechanical and thermal properties, etc. A systematic study of how membrane properties vary with preparation conditions will therefore be important for the rational design of process equipment and conditions for particular applications.

While the early literature on the subject [23–32] addressed fundamental and mechanistic aspects of IP reaction, the bulk of the literature is motivated by practical considerations. A fundamental understanding of the mechanisms involved, which can lead to rational models, is therefore difficult to arrive at, with few studies being available [33]. For example, while the time course of the polymerization has been studied either through film thickness [34,35] or monomer consumption [36–40], the evolution in time of various properties of importance has hardly been studied in the literature. Such studies can be of great value in validating models,

* Corresponding author. Tel.: +91 22 25767240; fax: +91 22 25726895.
E-mail address: aksuresh@iitb.ac.in (A.K. Suresh).

0032-3861/$ – see front matter © 2010 Elsevier Ltd. All rights reserved.
doi:10.1016/j.polymer.2010.01.004

and in estimating model parameters. Similarly, detailed information on the dependence of properties such as polymer molecular weight distribution (MWD), crystallinity and morphology on the various preparation conditions is hard to find. Finally, despite the interfacial nature of the process, the precise nature of the influence of parameters such as pH (which controls the availability of the aqueous monomer), interfacial properties and solvent remain unclear.

The present study is motivated by the above lacunae in the literature. In a recent paper [1], we have described a comprehensive model for IP and carried out detailed parametric studies on the model. The experimental studies described in the present paper are therefore also meant to validate the assumptions and predictions of the model. Here, we describe studies on a polyurea system (aqueous phase monomer: hexamethylene-1,6-diamine (HMDA) and organic phase monomer: hexamethylene-1,6-diisocyanate (HMDI)) with respect to influence of preparation conditions on polymerization kinetics and polymer properties. Preliminary experiments showed a need to refine the protocols used in previous studies for sample preparation, and accordingly, refinements have been carried out. A particular focus here is the MWD, a study of which is made difficult by the extreme insolubility of polyurea in most solvents. Here, we have employed HFIP (hexafluoro-2-propanol)-based GPC to characterize MWD and study the influence of various preparation parameters on the molecular weight and its distribution. The results have been used to derive the Mark–Houwink parameters for this polymer. Further, an attempt has been made here, for the first time, to follow the evolution of this and other properties during the course of the reaction. Several different characterization and analytical techniques such as FTIR, XRD, TG-DSC, SEM, viscometry, tensiometry and contact angle analysis have been used to gain insights into the mechanistic details of the process.

2. Materials and methods

2.1. Chemicals

HMDA and HMDI of purity >99% were obtained from Fluka, Switzerland and Merck, Germany respectively. Both were used without further purification. The organic solvents cyclohexane, carbon tetrachloride, p-xylene and toluene as well as 98% H_2SO_4 were purchased from Merck, India. Distilled water was used as the solvent for HMDA. The emulsifier Tween-85 (Fluka, Switzerland) was used to stabilize the o/w emulsions in which the reaction was carried out. The solvent used for GPC (gel permeation chromatography) analysis, HFIP (hexafluoro-2-propanol, purity >99%), was purchased from Apollo Scientific Limited, UK, and redistilled before use. Sodium trifluoroacetate (NaTFAc, procured from Fluka, Switzerland with a purity >99%) was added to the HFIP used in GPC analysis to suppress the formation of polymer aggregates because of the high polarity of the solvent. Polymethylmethacrylate (PMMA) standards, used in GPC for purposes of calibration, were purchased from Polymer Laboratories, UK.

2.2. Synthesis

Most of the experiments were directed at producing microcapsules, while a few experiments were conducted to synthesize polyurea as a flat film. The polyurea microcapsules were synthesized according to the procedure reported in the literature [38,40]. The course of the reaction was followed, as in the earlier work, by monitoring the aqueous phase pH as a function of time. A calibration plot of pH vs. concentration of HMDA allowed the conversion of pH data to monomer conversion, where necessary. At the end of the experiment, the microcapsules were filtered. In initial experiments, following earlier work cited above, the filtered microcapsules were washed with methanol and water 2–3 times, and dried in an oven at 70 °C for 12 h. It was however observed, that the procedure affected both the yield and the crystallinity values. Experiments to determine the reasons, in conjunction with XRD and GPC analyses, implicated the methanol wash, because the low molecular weight oligomeric species were dissolved and removed from the polymer. The scatter in the reported crystallinity values in earlier papers [40,41] could at least partly be because of this reason. Substituting methanol by the same organic solvent as was used in the synthesis solved the problem, as XRD and GPC analyses indicated the crystallinity and molecular weights to be insensitive to the number of washes given. This newly established sample preparation protocol was used in all the characterization studies carried out in this work.

Experiments on the kinetics of IP reaction were also carried out in microcapsular geometry by recording (online) the continuous phase pH as discussed in earlier work [38,40]. The IP reaction locale, solvent effect and regime were studied with the help of these kinetic runs.

Microencapsulation studies were carried out as a function of the bulk mole ratio of the monomers (R) and the number of moles of limiting monomer per unit volume of dispersed phase (n_L/V_d). A phase volume ratio (V_d/V_a) of 0.05 was employed in all experiments. For a given chemistry, the important dimensionless groups that control the course of reaction and property development, according to the model presented in Dhumal and Suresh [1], have been found to be a function of the above parameters. Table 1 shows the experimental conditions employed. Compared to experiments reported earlier [38,40], the present data covers exhaustively the mole ratio range of 0.2–4, with studies on solvent type and time course of development of properties being targeted at $R = 1$.

In addition to the microencapsulation experiments described above, experiments were carried out to produce flat films to facilitate morphological studies, in the apparatus schematically shown in Fig. 1. These experiments were carried out by layering the two (immiscible) monomer-containing phases, one on top of the other. Thus, an aqueous HMDA solution (0.05 M, 400 ml) and organic (cyclohexane) HMDI solution (0.05 M, 200 ml) were allowed to react for 55 h in a closed vessel (Fig. 1). A porous Teflon support placed at the interface made it convenient to lift the film at the end of the reaction. The film was washed and then taken for characterization.

Contact angle measurements, to understand the wetting characteristics of the IP film, needed a flat and even region of polyurea film. The flat films produced as above proved unsuitable for this purpose because of the low mechanical strength of the film. The films for contact angle measurements were therefore synthesized separately, with the same concentrations of monomers. In these experiments, the film was formed at the interface between the organic and aqueous phases, in a petri-dish. At the end of the reaction, after careful removal of the upper phase with a syringe, the formed film was broken from one side of the dish and a cover-slip

Table 1
Experimental conditions employed in the microencapsulation experiments ($V_d/V_a = 0.05, V_a = 110$ ml) (CH-cyclohexane, XL-p-xylene, TL-Toluene).

nL/Vd (kmol/m3)	R (mole ratio of HMDI/HMDA)							
	0.2	0.4	0.6	0.8	1	2	3	4
0.182			NSCH3-9		SCH9	NSCH9		
0.364			NSCH3-10		SCH10	NSCH10		
0.545	SCH1, RSCH1	SCH2	SCH3, RSCH3, NSCH3-15	SCH4	SCH5, RSCH5, XL5, TL5	SCH6, RSCH6, NSCH15	SCH7, RSCH7	SCH8
0.727			NSCH3-11		SCH11	NSCH11		
0.909			NSCH3-12		SCH12	NSCH12		
0.109			NSCH3-13		SCH13	NSCH13		
0.127			NSCH3-14		SCH14	NSCH13		

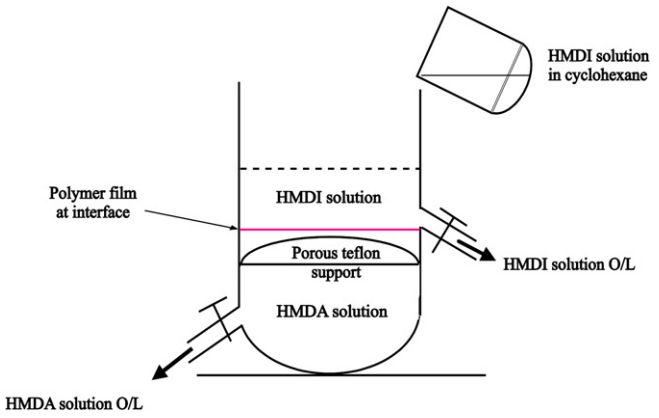

Fig. 1. Experimental set-up for flat polyurea film formation.

was inserted beneath the film to lift it off [42]. After careful washing with the same solvent and drying, the cover-slip was taken for contact angle studies. It was usually only the top surface that could be studied by this procedure. In order to examine differences between the organic and aqueous sides of the film therefore, different organic phases, heavier and lighter than water, had to be used. Thus cyclohexane was used as the solvent to study the organic side, while carbon tetrachloride was used to study the aqueous side.

2.3. Analysis and characterization

The polyurea in the above described syntheses was analyzed and characterized using different techniques as described below.

The polyurea from the microcapsules was analyzed by *Fourier Transform Infra Red (FTIR) Spectroscopy* on a Perkin–Elmer Spectrum One spectrometer by using KBr pellet method, to check for the presence of specific functional groups and bonds in the film. These studies were useful in gaining insights into some aspects of IP mechanism.

Crystallinity was determined by *X-Ray Diffraction (XRD).* XRD patterns from finely ground polyurea microcapsule samples were obtained on a Philips X'Pert PRO diffractometer using Cu target at a voltage of 40 kV and current of 30 mA. Scans were taken for a 2θ range of $5–50^0$ with a step size of 0.02. More details are available in Wagh et al. [40].

Gel Permeation Chromatography (GPC) was used for the determination of molecular weight distributions of synthesized polyurea. MWD of interfacial polymers have not been extensively studied in the literature. Interfacial polyureas in particular, pose special difficulties for MWD measurements because of their insolubility in most common solvents used for GPC. In our experiments, of the several solvents tried, only 98% H_2SO_4 and HFIP were able to dissolve the synthesized polymer to give clear solutions. HFIP was finally selected as the solvent for GPC. Before the analysis, HFIP from the market was redistilled. As HFIP is a highly volatile and expensive solvent, the condensate was collected in a chilled container to minimize losses. In addition to being volatile, HFIP is quite corrosive and care has to be taken in the interest of safe handling. The whole work was therefore carried out in a fume hood with proper safety precautions. The addition of NaTFAc salt in the highly polar HFIP is recommended to avoid agglomeration because of ionic interactions. Thus the mobile phase prepared for GPC use was HFIP containing 20 mM NaTFAc.

The GPC system itself was assembled from a Viscotek 1122 isocratic pump, a Shimadzu RID-6A (refractive index) detector and two HFIP-based columns (PL HFIPgel, 300 × 7.5 mm) along with a guard column. PMMA was used as calibration standard. The analyses were carried out at 30 °C and a flow rate of 0.7 ml/min of the mobile phase. A Jasco interface card was used to get online RI signal data from the RI detector. The recorded data was then analyzed using Borwin software to get the molecular weight distribution. The reproducibility of the GPC analysis was checked and found to be good, with chromatograms from repeat runs virtually overlapping with each other.

Thermo Gravimetry (TG) and *Differential Scanning Calorimetry (DSC)* studies, in order to study the crystallization characteristics of the polymer samples of interest, were carried out on a *Simultaneous Thermal Analyzer* (STA 409 PC Luxx, Netzsch, Germany). Samples weighing 2–6.5 mg were heated in the thermal analyzer from 30 to 400 °C in a platinum pan at a constant heating rate of 10 °C/min under a N_2 atmosphere for these studies. Some determinations were repeated on a DuPont 2000 machine with aluminum pans, for confirmation.

The determination of *Intrinsic viscosity* of the polymer solutions in 98% H_2SO_4, for the purpose of establishing the Mark–Houwink constants, was carried out in an Ubbelohde viscometer, at a constant temperature of 23 °C, by the conventional procedure of measuring the solution efflux time and that of the pure solvent. The concentration of the polymer sample used was 0.5 g/dl (0.005 g/ml). The intrinsic viscosity of polymer solutions was calculated by the one point determination method described by Kinsinger [43]. Each measurement was repeated three times.

Morphological studies were carried out on a JEOL JSM-6400 *Scanning Electron Microscope (SEM)* at 10 kV after coating the samples with gold. For studying the cross section, a section of the film was taken carefully using a sharp blade and mounted vertically on a carbon tape.

Interfacial tension and contact angle (polyurea film) measurements were performed on a GBX – 3S tensiometer with contact angle measurement accessory (Digidrop). The Wilhelmy plate method was used for the interfacial tension measurements. Each measurement was repeated three times. Care was taken in these studies to wash the glassware thoroughly with chromic acid, since even a slight impurity can affect the interfacial tension values greatly. The contact angles were measured at 7–8 different locations and an average taken.

3. Results and discussion

3.1. Process kinetics

A detailed process kinetics study of polyurea formation was reported in our recent work [40], with the help of continuous phase pH measurement. In that work the kinetics were analyzed by plotting the drop in pH, namely $(pH_0 - pH)$, with time. It was shown that the presence of a linear region (after an initial period of adjustment) on such a plot is indicative of an overall first-order dependence of the rate of consumption of the diamine monomer on its concentration. Further, a strong dependence of the slope of this line on the organic side conditions would indicate (a) that the reaction is on the organic side of the interface and (b) that the reaction is kinetically controlled. Fig. 2 shows the effect of the organic phase monomer (HMDI) concentration on the rate of consumption of HMDA. In these runs, the HMDA concentration was the same but the HMDI concentration was varied to vary *R*. With increase in *R*, i.e. increase in the HMDI concentration in the organic phase, the kinetics is seen to be accelerated. That the IP reaction for microcapsule formation is often kinetically controlled has also been inferred by Yadav et al. [38] by a comparison of their experimental results with a lumped model which treated the resistances due to diffusion and kinetics.

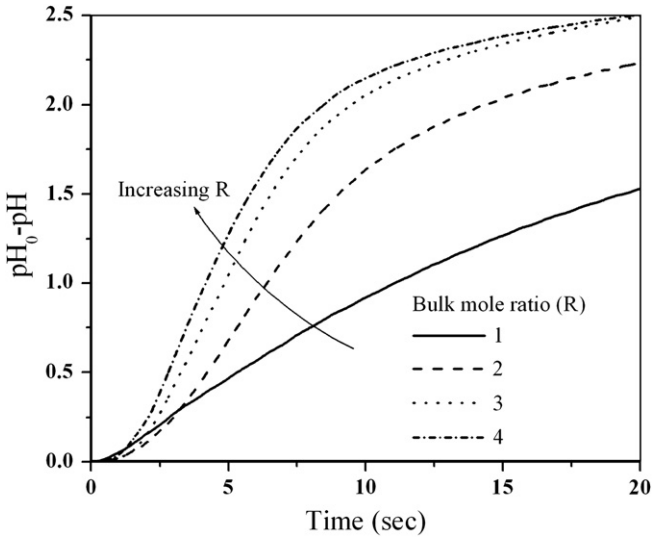

Fig. 2. Effect of the monomer mole ratio of HMDI to HMDA (R) on process kinetics ($n_L/V_d = 0.545$ kmol/m^3).

Data such as the above have been used to estimate the parameters in the model described in our earlier work [1]. The parameter estimation procedure discussed by Dhumal et al. [44] is used here along with the physicochemical parameters/constants of the system mentioned in our previous work [1]. Since the above data suggest kinetic control, diffusivity of aqueous phase monomer through the IP film ($D_{A0} = 5 \times 10^{-12}$ m^2/s) was not fitted but kept fixed at the value taken from our earlier work [44], and the reaction rate constant fitted by matching the experimental and theoretical curves. The match, for different values of R, is shown in Fig. 3. A value of 6000 m^3/kmol s was found to fit the data for $R > 1$. The comparison shown for $R = 1$ is with this value of k. While the fit is found to be satisfactory up to about 80% conversion for $R > 1$, the data for $R = 1$ would seem to require a higher value for the rate constant than $R > 1$. Discrepancies between theory and experiment in the 80–95% conversion region, for cases of $R > 1$, were also found by Dhumal et al. [44], who speculated that the discrepancy could be due to variations in diffusivity during the run thus calling into question the assumption that kinetic control prevails throughout the run. However, calculations of the diffusion–reaction parameter proposed in Dhumal and Suresh [1] with the fitted value of k shows that the conditions of kinetic control are unlikely to be violated for this case, even if the value of diffusivity were to change by a large magnitude. The discrepancy after 80% conversion is therefore believed to be due to other causes. A strong possibility is that of an end-capping reaction within the film, not considered in the model, which consumes HMDA as it diffuses through the film.

An end-capping reaction such as suggested above would also explain the poor fit of the theory with experiment for the case of $R = 1$. The model of Dhumal and Suresh [1] shows that in general and particularly if the chains are not very long, the diisocyanate is consumed at a faster rate than the diamine. On this basis, it predicts that a complete conversion of monomer A is not possible for $R = 1$, as the theoretical curve in Fig. 3 shows. Experimental data on the other hand, show that the diamine is completely consumed for this case. The possibility of a film reaction, by bringing in an additional mechanism for the consumption of monomer A, would therefore reconcile the two. The lack of fit is thus seen to be a consequence of the fact that the theoretical prediction is tending towards a lower asymptotic value from the start. The problem of the asymptote is not present for values of $R \geq 2$, since the model predicts complete conversion of the diamine [1]. The possibility of an end-capping

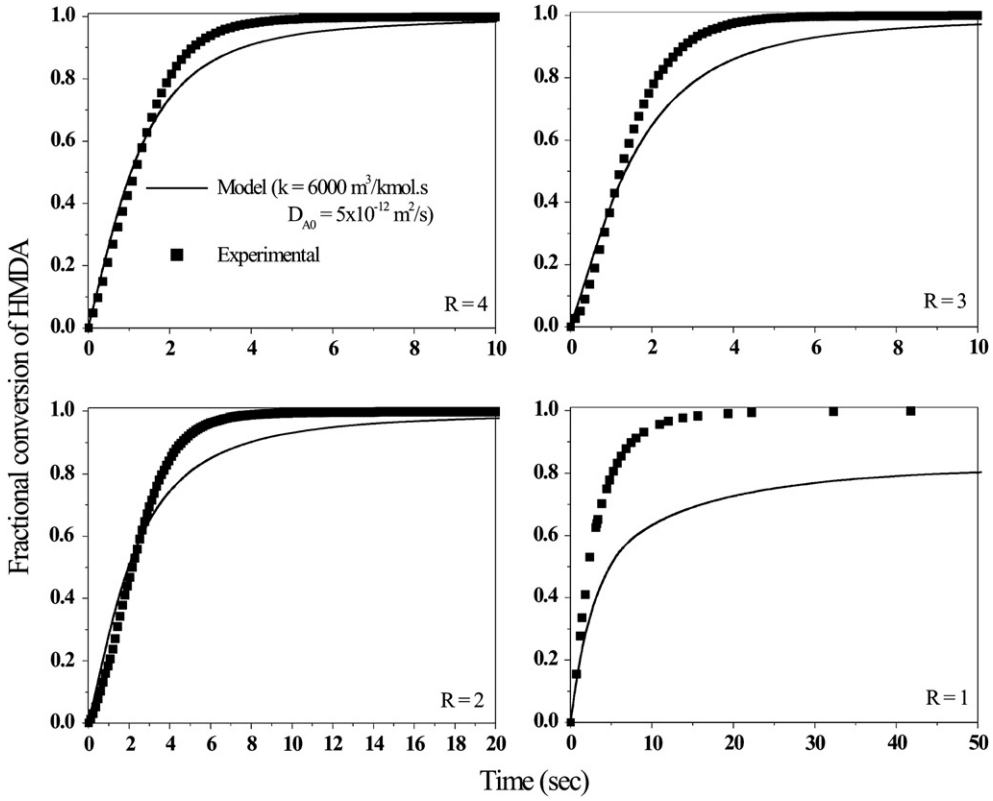

Fig. 3. Conversion-time behavior with cyclohexane solvent ($R = 4$, $n_L/V_d = 0.545$ kmol/m^3): Comparison of model with experiment.

reaction in the film is explored in some detail in the following sections, through FTIR studies.

The rate constant reported with cyclohexane solvent in this work is about half of what was reported in the earlier study of Dhumal et al. [44] which used an empirical model for the nucleation rate. A more fundamentally-based model for nucleation, used in Dhumal and Suresh [1] necessitates the assumption of a reaction zone that is twice as thick as that assumed in Dhumal et al. [44]. This difference in the size of the reaction zone explains the lower value of the rate constant, when the kinetic data are fitted to the model of Dhumal and Suresh [1].

3.1.1. Solvent effect on kinetics and interfacial properties

Wagh et al. [40] found that the solvent used for HMDI had a significant influence on the kinetics. For the four solvents that they used, they found the rate constants to be in the order cyclohexane > p-xylene ∼ carbon tetrachloride > toluene. Experiments repeated for different values of the parameter n_L/V_d as part of this work confirm this trend. Fig. 4(a and b) shows the conversion-time data with p-xylene and toluene under otherwise the same conditions as the curve for $R = 1$ in Fig. 3. The predictions fall below the experimental at high conversions, as above, but the early part of the experiments yield the values for the rate constants shown in the figure.

While a simplistic understanding of the solvent effect would expect the rates to be proportional to the solubility of the aqueous phase monomer in the solvent, the order of rate constants observed in these studies goes against the order of equilibrium amine concentration in the solvent (calculated on the basis of partition coefficients). Wagh et al. [40] showed that the relative magnitudes of rate constants correlate with the dielectric constants of the solvents and invoked one of the Hughes–Ingold rules in an attempt to explain this. An effort was made in this work to see if the heterogeneous nature of the reaction, and the presence of a phase-interface, can explain the observed trend. Thus, the tendency of the monomers to adsorb at the liquid–liquid interface was studied through interfacial tension measurements. This would also throw some light on the role of the interface in IP in general, since this has been a debated issue in the literature. Starting with Morgan [23], many previous researchers have speculated on the role of the interface – whether it serves merely as a diffusion barrier or whether it is the site of reaction [45]. Interfacial tension studies would be important from the point of view of applications of IP as well since, in some applications (e.g. microencapsulation), a surfactant is present during the synthesis while in others (e.g. TFCM), no surfactant is used. The nature of the interface will clearly be different in the two cases and it would be of interest to know what difference, if any, this would make to the progress of the reaction.

Table 2
Interfacial tension (I. T.) studies of IP system at 27 °C.

Solvent (S)	Water/S I.T. (mN/m)	I. T. with Tween 85 (mN/m)	I. T. with Tween 85 and HMDA (mN/m)	I. T. with Tween 85 and HMDI (mN/m)	I. T. with HMDI only (mN/m)
Cyclohexane	49	9.56 ± 0.07	8.19 ± 0.04	8.73 ± 0.01	23.25 ± 0.20
p-Xylene	35	10.28 ± 0.15	9.93 ± 0.04	9.48 ± 0.25	25.59 ± 0.01
Toluene	36	11.66 ± 0.17	10.73 ± 0.07	10.69 ± 0.11	23.97 ± 0.53

Since in situ monitoring of the interfacial properties of the system during reaction was not possible on practical grounds, the interfacial tension of the IP system (aqueous HMDA phase and organic HMDI phase, in the presence and absence of Tween 85 emulsifier) was determined in this work under conditions of no reaction, by excluding one or the other of the monomers. Determinations were carried out with the help of GBX Tensiometer and Wilhelmy plate method. The average values of system interfacial tension are reported in Table 2. The interfacial tension between organic and aqueous phase for all three solvents in presence of Tween 85 emulsifier (4% v/v) was found to be around 10 mN/m. The monomer concentrations used during interfacial tension study are the same as used in the study of solvent effect on kinetics. Before interfacial tension measurements with aqueous HMDA solution, the solution was allowed to equilibrate with the organic phase for a minimum of 2 h. This could not be done for cases in which a HMDI solution was to be contacted with water, because of the possibility of hydrolysis, and determinations were carried out soon after contacting. This was satisfactory since HMDI is not expected to partition into the aqueous phase in any case. The possibility of the hydrolysis reaction occurring to any appreciable extent during the course of the measurement is small, since the interfacial tension measurement took only around 10–15 min and the rate of the hydrolysis reaction is quite slow [38,46,47].

The results of these measurements are summarized in Table 2 for the three solvents used, cyclohexane, p-xylene and toluene. The table shows that in general, the monomer (whether HMDI or HMDA) makes a difference to the interfacial tension only in the absence of a surfactant, the interfacial tensions being unaffected when the emulsifier is present. The surfactant, by virtue of its greater affinity for the interface, seems to effectively exclude the monomer from the interface. Thus, the importance of interfacial reaction, if any, would be negligible in those situations (e.g., microencapsulation) where a surfactant is present. By the same token, in such situations, one

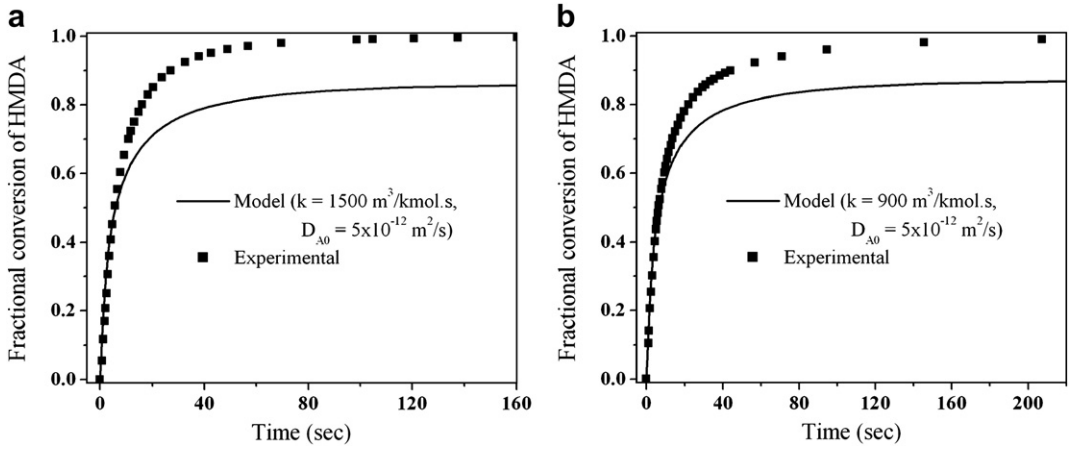

Fig. 4. Conversion-time behavior with (a) p-xylene and (b) toluene solvent ($R = 1$, $n_L/V_d = 0.545$ kmol/m^3, $k'_m = 1.5 \times 10^{24} \#/m^3$s): Comparison of model with experiment.

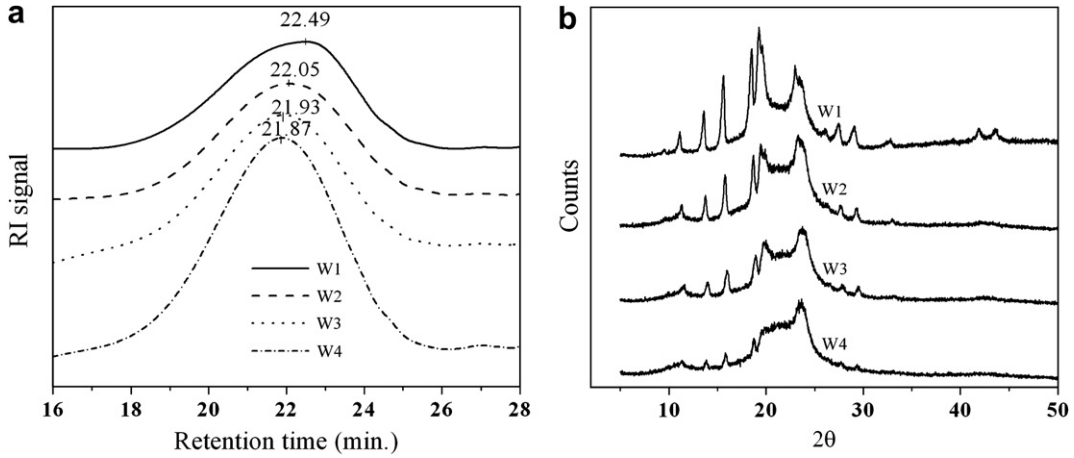

Fig. 5. (a) GPC and (b) XRD analysis of methanol washed samples.

would expect the solvent to exert the same influence in IP as it would in homogeneous reaction. While homogeneous kinetics have not been determined for the polyurea system, it may be mentioned that for the polyamide system, Morgan [23] shows that solvent effect in IP is the same as in homogeneous kinetics.

Having thus decided that the bulk properties of the solvent are what are important in explaining the differences due to the solvent in the present work, several relevant properties such as viscosity, dipole moment, dielectric constant and diffusivity of the diamine were-examined for the solvents used. The observed order of reactivities best correlated with the dielectric constant as found in our earlier work [40], and this is consistent with the Hughes–Ingold rules. A more quantitative comparison with these rules would require consideration of the charge density of the activated complexes that form and interactions with the solvent.

3.2. Polymer properties

3.2.1. Sample preparation protocol for characterization studies

While the previous work followed a sample preparation protocol that involved methanol washes, this procedure was re-examined in the light of a high scatter in the property values, especially crystallinity, obtained under certain conditions. The polyurea microencapsulation experiment was repeated several times with same preparation conditions (R = 0.9415, n_L/V_d = 0.505 kmol/m^3, V_a = 110 ml, V_d/V_a = 0.0484) but with different washing protocols. The washing of filtered polyurea microcapsules is necessary to remove any unreacted moieties. The results for MWD and crystal structure, after repeated washes with methanol, are shown in Fig. 5(a and b). Fig. 5(a) shows that, with every wash, the MWD becomes narrower and shifts to higher molecular weights, indicating the progressive removal of low molecular weight material. Determination of polymer yields in these cases showed that the quantity of polymer recovered also decreases with every wash, a finding which is consistent with the above conclusion. That this results in a change in the overall crystalline structure also, is clear from Fig. 5(b).

The use of methanol wash in sample preparation was therefore discontinued. Instead, the same solvent as was used in the synthesis was used to wash the capsules and remove any adhering monomer. Fig. 6(a and b) illustrates the results after several cyclohexane washes, in a run in which cyclohexane was the solvent. Clearly, there is no change in sample characteristics even after several washes.

3.2.2. Chemical nature of the film formed

Fig. 7 shows an FTIR scan of the IP film (R = 4, n_L/V_d = 0.545 kmol/m^3). The peak at 3353 cm^{-1} indicates the hydrogen bonded N–H stretching. The C–H stretching vibrations of –CH_2 groups are observed between 3000 and 2800 cm^{-1}. The strong stretching vibration seen near 1627 cm^{-1} is caused by C=O stretching; this is followed by one more N–H peak at 1578 cm^{-1}. The presence of the –NCO group is indicated by the stretching vibration found around

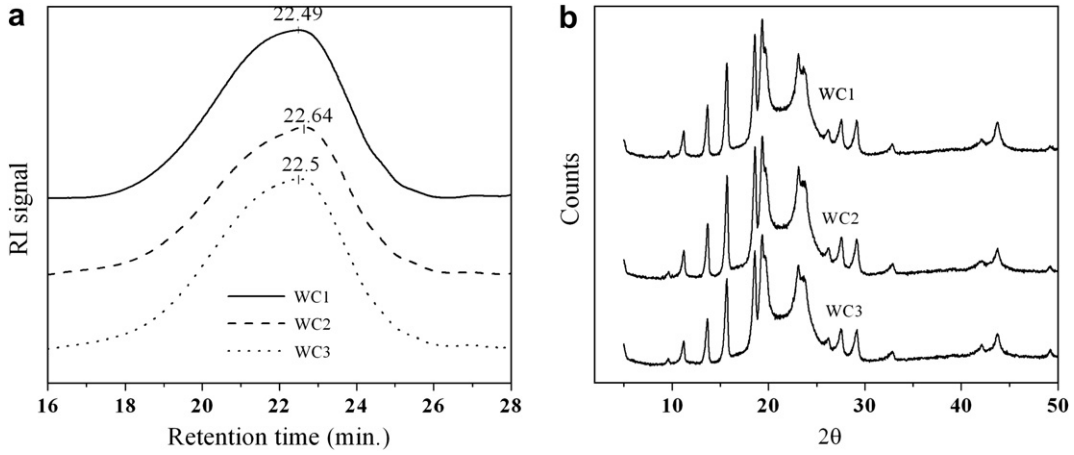

Fig. 6. (a) GPC and (b) XRD analysis of cyclohexane washed samples.

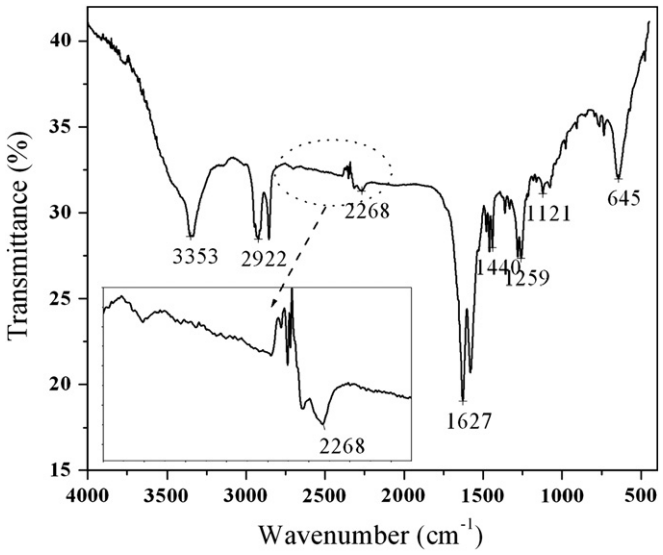

Fig. 7. FTIR spectrum of polyurea sample (SCH8).

2268 cm^{-1}. The FTIR scan is thus typical of bonds expected in polyurea.

3.2.3. Morphology and surface characteristics

Since attempts to investigate the morphological features of the two faces of the IP film in microcapsules were not very successful, such a study was carried out on the flat films produced as described in the Section on synthesis methods. The morphology of the organic and aqueous faces of the polymer film can give some insights into the locale of reaction – whether on organic or aqueous side of the interface [23,48,49]. The change in morphology along the thickness of the film shows the history of film formation. Fig. 8 shows the SEM micrographs of the aqueous side of the interface (8a), cross-sectional view (8b) and organic side (8c) of the polyurea film. The presence of small globular structures on the surface, much more numerous on the organic side than on the aqueous, is an interesting feature of these micrographs. The cross-sectional view of the film shows a distinct difference between the dense first-formed film and later accumulation, and suggests that the formation of these globular structures starts just after the initial film formation event. The film thickness, after 55 h of reaction, was in the range 8–12 micron. The globular microstructure has been commented on in the literature, and one sees two different opinions as regards the causes. According to Cadotte et al. [48], the formation of spherical globules suggests mixing at the interface, resulting in an emulsion formation. Some local contractions and expansions were found at the liquid–liquid interface by Nakache et al. [50], suggesting such a possibility. According to Janssen and Nijenhuis [34], the aqueous phase which swells, and diffuses through, the membrane forms drops on the organic side, on the surface of which polymerization continues. The mechanism has to remain speculative for now, but certain other features of the flat films are worth noting. This film was found to be insoluble in HFIP even after it was kept for three to four months in HFIP, suggesting the presence of molecular weights much higher than in the microencapsulation experiments. According to Morgan [23] the intrinsic viscosity of the product decreases with an increase in interfacial area. The interfacial area in the flat film experiment was 6.36×10^{-3} m^2, much lower than in the microencapsulation experiments (27.5 m^2, 4322 times larger). The model prediction of the polyurea film properties formed under these conditions was

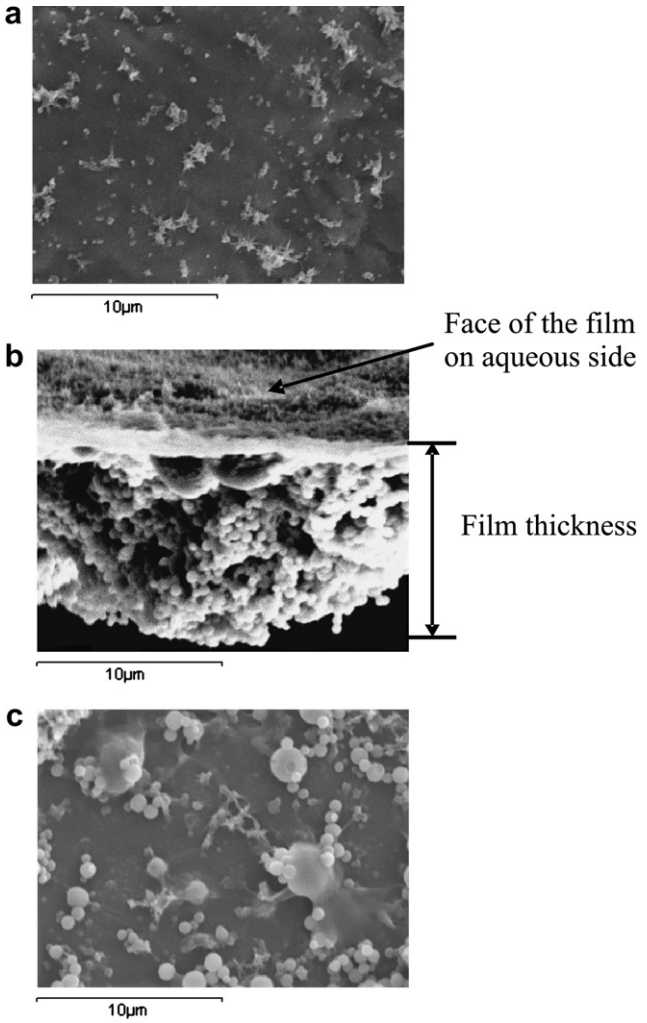

Fig. 8. SEM micrographs of the polyurea film: (a) Aqueous side, (b) cross-section and (c) organic side. Images were taken with 3000X zoom and scale bar is 10 micron.

difficult because the computations became highly intensive – satisfactory closure of material balance for these cases required consideration of much higher values for the maximum chain length. The model thus lends a qualitative support for the formation of high molecular weight material under these conditions.

Polyurea films, formed in a petri-dish and collected on a glass slide as described earlier, were analyzed for wetting characteristics by using a contact angle analyzer. With adequate care being taken in sample preparation as detailed before, the contact angles measured at several locations on the film were usually within 1–2°. The contact angles on the two sides of the film were found to be different, the rough organic side showing a higher contact angle (98°) than the smooth aqueous side (80°). This may be either due to the differences in roughness or to a higher abundance of the amine ended oligomeric species on the aqueous side. In general, the aqueous side seems to have enough hydrophilicity to allow ingress of that phase and diffusion of HMDA. These results also suggest an anisotropic nature of the IP film.

3.2.4. Polymer yield

The thickness of the polymer film formed is an important parameter that affects the performance of the film. Since determination of the thickness of the film in microcapsules was difficult, the next best thing was done by determining the polymer yield.

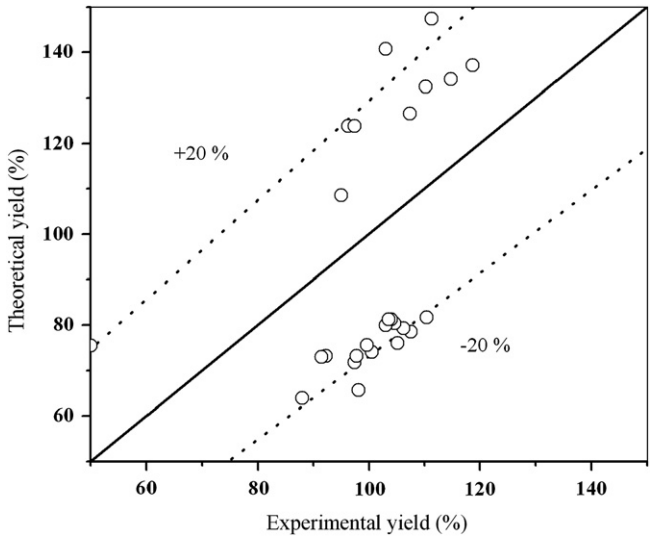

Fig. 9. Comparison of polymer yields in microencapsulation.

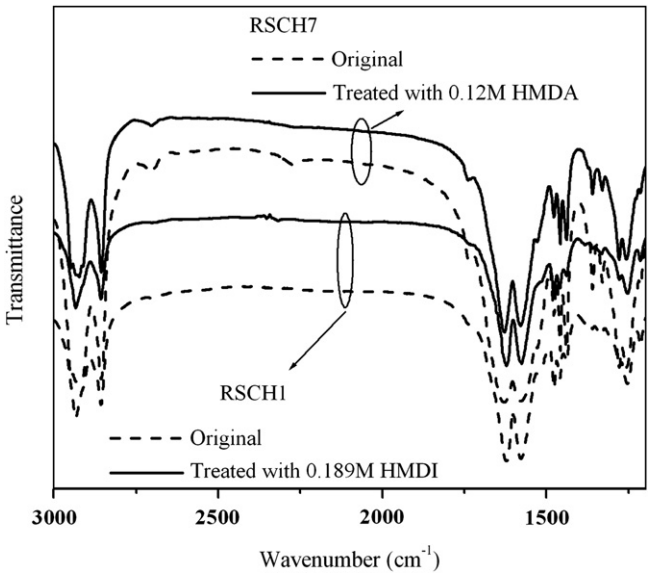

Fig. 11. FTIR spectra of polyurea sample RSCH1 (n_L/V_d = 0.545 kmol/m^3, R = 0.2) and RSCH7 (n_L/V_d = 0.545 kmol/m^3, R = 3), showing the effect of post-treatment.

Experimentally, the yield was measured by weighing the final dried polyurea product, and expressing this as a fraction of what is expected based on complete consumption of the limiting monomer (HMDA for $R > 1$ and HMDI for $R < 1$) and a 1:1 stoichiometry. As shown by Dhumal and Suresh [1], the actual stoichiometry of monomer consumption will in general be different from 1:1, and has a limiting value of 1:2 (HMDA:HMDI). Fig. 9 compares experimental yields so calculated with yields predicted by the model. Model calculations require values of the rate constant, diffusivity and nucleation rate constant to be specified. While the values of the first two have been given above, the value of the nucleation rate constant has been determined as will be explained in further paragraphs, from the time course of development of crystallinity. Further, theoretical calculations only include the part of the polymer that has finally been incorporated into the film, and not the part of the polymer that remains dissolved.

Fig. 9 shows that in general, the agreement between experimental and theoretical yields is within 20%. Fig. 10 shows this comparison as a function of preparation parameters, and show that the trends are well captured by the model in a qualitative sense. Quantitatively, it is observed that theoretical estimates are usually higher for $R > 1$ and experimental yields are higher for $R < 1$, the discrepancy between theory and experiment being larger for the latter case. Experimental yields would be expected to be higher than theoretical for cases of excess diamine ($R < 1$), if the possibility of end-capping of the polymer chains by reaction in the film, as explained earlier, is considered. This gives a partial explanation of the trends observed.

The possibility of an end-capping reaction in the film, which results in a consumption of HMDA by reaction with the –NCO end-groups in the film, can be confirmed by treating the polymer with HMDI and comparing the FTIR spectra before and after such treatment. Fig. 11 shows the effect of such a treatment, for a film formed under conditions of R = 0.2 (other conditions are mentioned in the figure). Although the mole ratio shows an excess

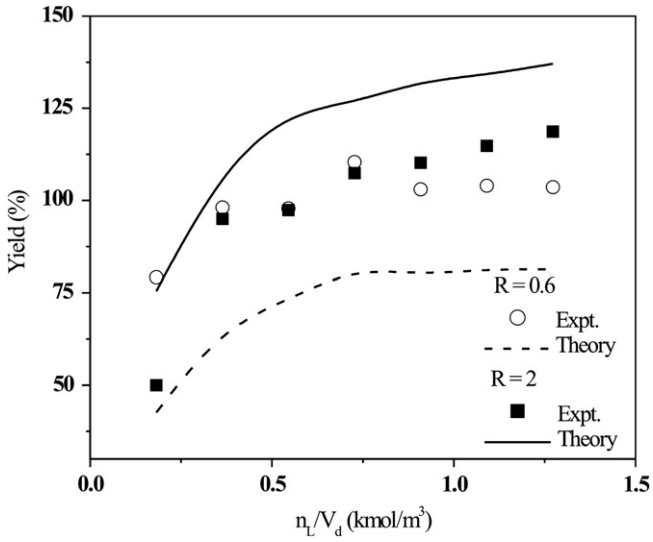

Fig. 10. Comparison of polymer yields in microencapsulation.

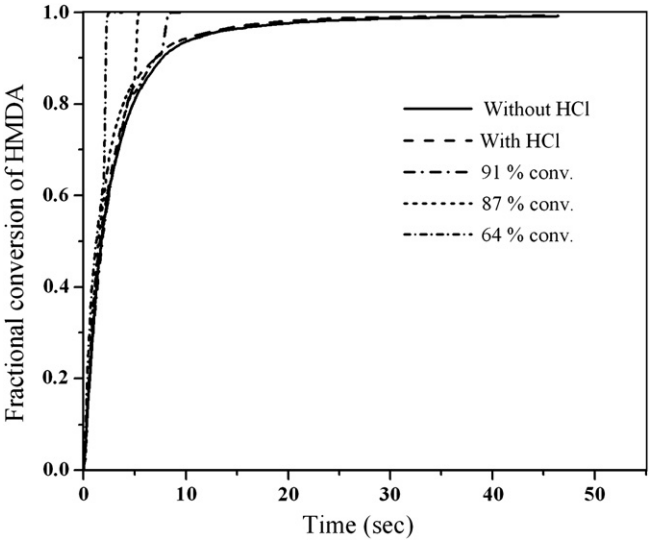

Fig. 12. Conversion-time plots for the experiments carried out to different extents to study the development of polymer properties with time (run 1).

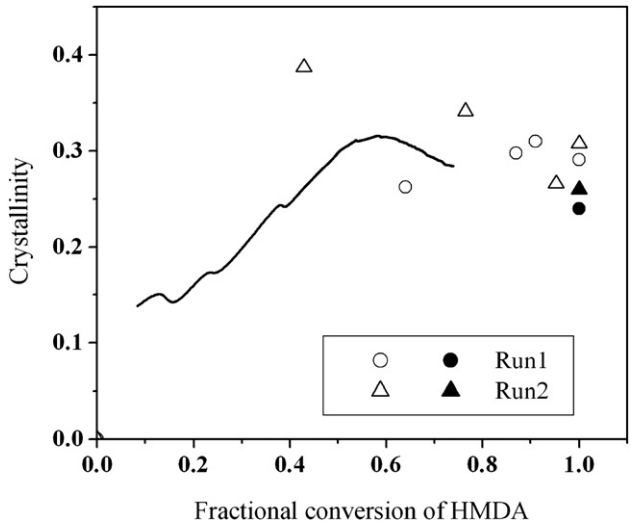

Fig. 13. Time variation of polymer crystallinity ($R = 0.9415$, $n_L/V_d = 0.505$ kmol/m^3, $V_a = 110$ ml, $V_d/V_a = 0.0484$): Comparison of model with experiment (the dark symbols corresponds to the end-of-run crystallinity after HCl charge).

of HMDA by a factor of 5, model calculations indicate that in the reaction zone, there is a dominance of isocyanate-ended oligomers; the other types of oligomers are at negligible concentrations. One would therefore expect the film to contain mostly the isocyanate-ended chains. The FTIR spectrum however shows no peaks characteristic of –NCO in the 2270 cm^{-1} region. On the other hand, when this film is treated with HMDI for 2 h, the spectrum shows a clear evidence of these groups. This indicates the presence of significant numbers of amine end-groups, which are converted into –NCO as a result of treatment with HMDI. From the foregoing, it is clear that these groups could only have resulted as a reaction of the diffusing diamine with the –NCO end-groups on the precipitating chains, during synthesis.

Fig. 11 also shows the result of a similar study for a film formed at $R = 3$, i.e., with an excess of diisocyanate in the recipe. The film as formed in this case, does show the presence of –NCO groups. A treatment with HMDA gets rid of these peaks, confirming that they were of –NCO groups. This is possibly from the contributions of the isocyanate-ended polymer formed towards the end (when the amine monomer is nearly completely exhausted). Further confirmation of this can come if the polymer formed in intermediate stages can be examined for the presence of –NCO groups.

3.2.5. Crystallinity: variation during synthesis and estimation of nucleation rate constant

Following the development of polymer property as a function of time during the reaction can give important insights into the influence of different factors on the progress of the reaction. This information can also be used to fit those parameters in simulation models that control property development. In the model of Dhumal and Suresh [1], the nucleation rate constant is such a parameter. In this work, the development of properties with time was followed by stopping the reaction at different stages, by a sudden lowering of pH by dumping HCl (10 ml of 1 M) into the reaction mixture. Since only the unprotonated form of the diamine can take part in IP reaction, protonation of the diamine would stop the reaction. The capsules can then be filtered, washed and taken for characterization in the usual manner. Fig. 12 shows the conversion-time plots (generated from the measured variation of pH) for five experiments carried out for this purpose. All these experiments were started with identical conditions. In three of these, the reaction was quenched at intermediate stages by HCl addition as described above. Two reactions were allowed to go the full distance, and in one of these HCl was added at the end to see the effect, if any, of such addition on the properties measured. This entire set of experiments is designated as one run for the purpose of studying property development with reaction time. Two such runs were carried out to check reproducibility, although the reactions could not always be stopped at the same conversions in the two sets.

Fig. 12 shows a good reproducibility of the conversion-time behaviour in the experiments within a run – the samples of polymer from the different experiments within a run could therefore have come from the same experiment. As seen in this figure, the reaction was stopped at 64, 87 and 91% conversions respectively, in this run. Fig. 13 shows the variation of polymer crystallinity with conversion (time), as determined from the two runs. The figure also shows the model calculations for a value of the nucleation rate constant that provides a good fit to the data. As seen, the theory [1] anticipates an initial increase in crystallinity with a slight drop towards the end, as spinodal decomposition becomes dominant towards the later part of the run. While such a trend was clearly seen in one of the two runs (the one represented by open circles in Fig. 13), a degree of qualitative agreement is seen between the theory and experimental data in general. Several points are in order with regard to this comparison. Firstly, it is seen from the end-of-run samples that HCl addition tends to lower the measured crystallinity by a few percentage points. If the reaction is allowed to end by itself without HCl addition, the swollen film is in effect allowed to age for a reasonable length of time (usually at least several

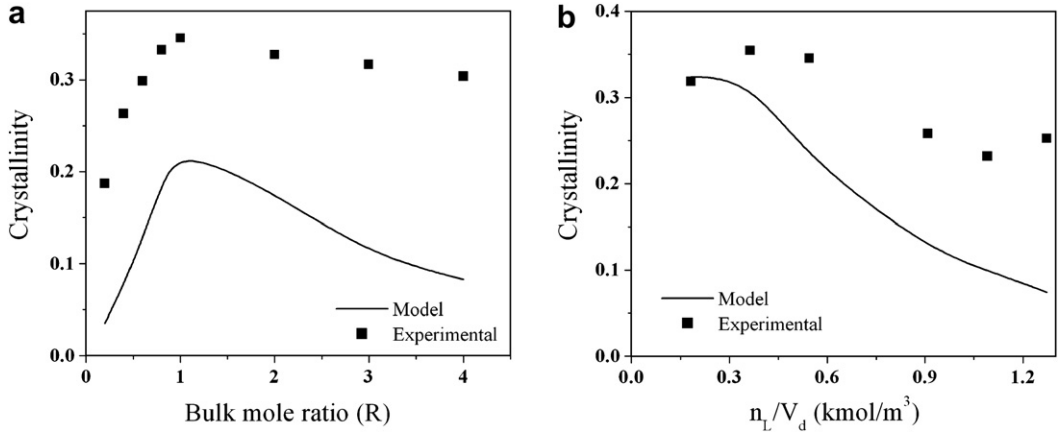

Fig. 14. Comparison of model predictions of crystallinity with experiments: Effect of (a) R ($n_L/V_d = 0.545$ kmol/m^3) and (b) n_L/V_d ($R = 1$).

minutes before separation). It has been shown through DSC studies [40,51] that the as-formed crystallinity in IP is lower than the maximum crystallinity achievable, and it is possible that such aging allows an improvement in the crystallinity towards the equilibrium value. It is also possible that any remaining supersaturation at the end of the reaction is discharged by a nucleation/growth process sufficiently slowly in the absence of HCl addition, so that the phase separated material achieves the crystallinity allowed by the chemical structure. HCl addition on the other hand, leads to a sudden precipitation of this material, which therefore will likely be amorphous. The second point refers to the theoretical calculations stopping short of 100% conversion, the reason for which, as argued thus far, is most likely to be the noncognizance of the reaction in the film.

Based on the fit shown in Fig. 13, the nucleation rate constant k'_m in the model of Dhumal and Suresh [1] is found to be around 1.5×10^{24} #/m^3 s. This is the value that was used in the yield calculations shown in Figs. 9 and 10.

3.2.6. Crystallinity: effect of experimental parameters

Crystallinity of the film is an important attribute since it strongly influences the permeability through the film. A significant finding of the previous work [7,51] on polyurea microcapsules was the fact that the crystallinity, and through it the permeability, could be varied considerably for the same chemistry. Previous work has established that the crystallinity of the film as formed is decided by experimental conditions, and is in general lower than the equilibrium crystallinity. There is thus an opportunity here for designing the capsule wall for a required permeability. The model of Dhumal and Suresh [1] allows a prediction of the as-formed crystallinity, taking the realization of this opportunity a step further. It would therefore be instructive to examine the ability of the model to describe the influence of experimental variables on this important property.

The experimentally observed effect of n_L/V_d and R on crystallinity is shown in Fig. 14 along with the predictions of the model. The value of k'_m estimated from the time variation of crystallinity at $R = 1$ has been used in the predictions. A good qualitative agreement is seen between the model predictions and data, in the case of both variables. Quantitatively, the model predictions are lower than the experimental values, but it has to be considered that the estimate of nucleation rate constant is based on limited amount of data on the time course, and at one value of R. It is also possible that the experimental crystallinities are a little higher because of aging and other factors discussed in the previous section.

Yadav et al. [51] and Goyal and Suresh [41] speculated on the existence of an inverse correlation between initial reaction rate and crystallinity. Since the initial reaction rate is proportional to the product of initial monomer concentrations, crystallinity data from the present experiments are plotted against this product to test this hypothesis in Fig. 15. The error bars show that the reproducibility of these measurements was satisfactory. The cases represented cover one or the other monomer being in excess, and the case of stoichiometric equivalence. While in general, an inverse correlation is seen, crystallinity is seen to be affected in a complex manner by several factors, and the correlation depends on the values of other experimental parameters such as n_L/V_d and R. Model predictions, also shown in the figure, are able to capture the trends qualitatively.

The extent to which the experimental conditions limit the ability of the polymer chains to crystallize can be followed using DSC on the as-formed polymer, which shows a cold crystalline transition just below the melting transition, under conditions of increased mobility of the polymer chains in the film [7]. While crystallinity is governed by a number of factors, the analysis of Dhumal and Suresh [1] shows that chain length is a dominant factor in determining crystallinity. It is therefore of interest to see whether we can get further insights by thermal analysis of the formed films.

Fig. 16 shows the DSC scans of several polymer samples, which differ in their molecular weights (a detailed discussion of molecular weights follows in the next section). The preparation conditions are shown in the figure. A lowering of the crystallization temperature (T_C) with molecular weight is clear. As the chain mobility increases with temperature, shorter chains find it possible to achieve crystalline order at lower temperatures than longer chains. This further confirms the suggestion in the literature that the crystallinity achieved during the synthesis in such systems is not limited by chemistry, but by the time available for crystallization.

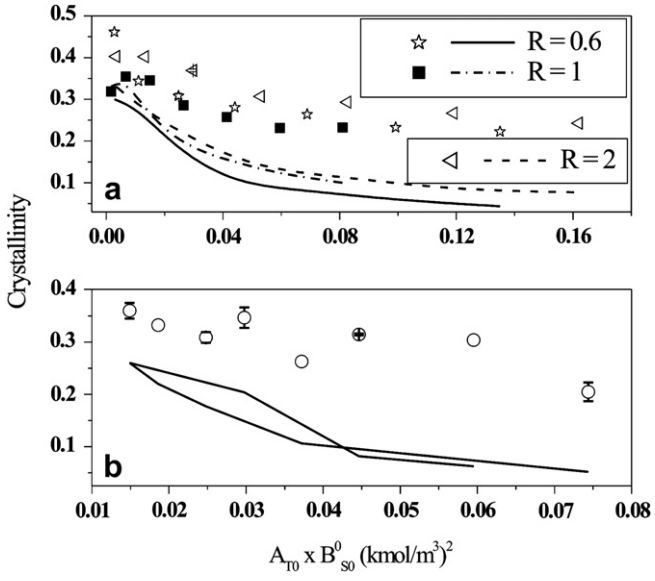

Fig. 15. Crystallinity plotted as a function of the product of initial monomer concentrations, to show the effect of initial reaction rate. In (a) the initial rate is varied by varying n_L/V_d keeping R constant (three values are shown), while in (b) the initial rate is varied by varying R, keeping n_L/V_d constant (0.545 kmol/m^3).

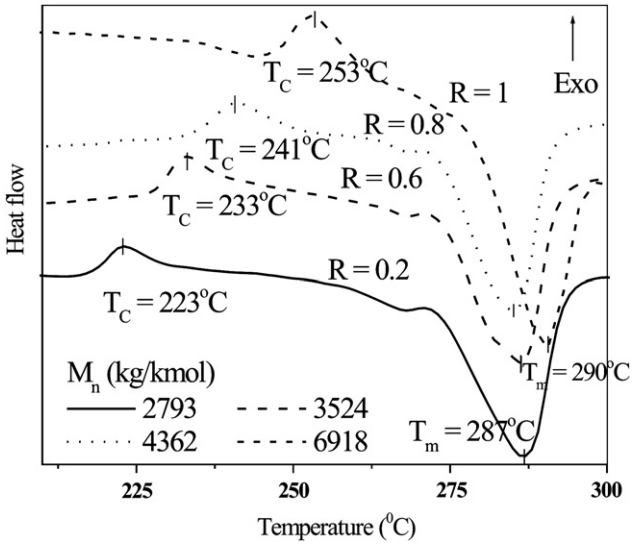

Fig. 16. Effect of molecular weight on crystallization temperature (n_L/V_d = 0.545 kmol/m^3).

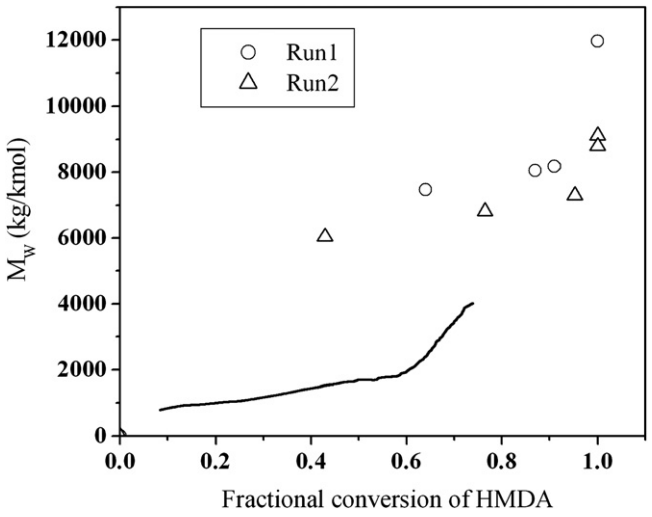

Fig. 17. Time variation of MWD ($R = 0.9415$, $n_L/V_d = 0.505$ kmol/m^3, $V_a = 110$ ml, $V_d/V_a = 0.0484$): Comparison of model with experiment.

3.2.7. Molecular weight: evolution with time

The development of molecular weight during the course of the reaction was followed in the same set of experiments as was described in connection with crystallinity. The results are shown in Fig. 17. The reproducibility of the data from the two runs is seen to be good in general. Molecular weight is found to increase monotonically with conversion, and the model also predicts this trend. The reasons for the model predictions stopping short of complete conversion have been analyzed earlier. The gradual increase in molecular weight with conversion is typical of step polymerizations in general, and is seen to be true even for the interfacial case.

3.2.8. MWD: general characteristics and effect of experimental variables

Fig. 18(a and b) shows the general characteristics of MWD of polyurea samples. Cases of $R < 1$ (diamine in excess) and $R > 1$ (diisocyanate in excess) are shown separately. The experimental data show a shift in the peak towards higher molecular weights as R increases. Fig. 18(c) shows the model predictions for the MWD for some of these cases, and the similarity in the general nature of the distributions with the experimental ones is clear. Both experimental and theoretical distributions are skewed with a long tail at the high molecular weight end. The presence of a shoulder past the mode of the distribution for small values of R, and its disappearance as R increases, are seen in both theoretical and experimental distributions. The theoretically predicted MWD shows better agreement with experiments at low values of R. At high R values, the MWD predicted by the model is narrow and the average, much smaller than found experimentally.

The average molecular weights M_w and M_N can be obtained from the MWDs obtained as above, and polydispersity values can be calculated. Fig. 19 shows the variation of weight average molecular weight M_W and polydispersity with R. Experimentally, M_W and polydispersity are found to increase continuously with increasing R. The reproducibility of these values was found to be good when the same stock of HMDI was used. As the lines representing the model calculations show, the model predicts the molecular weights to increase as R is decreased, while the experimental data show otherwise. As pointed out by Morgan [23], the concentration ratio of the monomers at the site of reaction is what determines the molecular weight, and conditions that tend to push the concentration ratio towards stoichiometric equality favour high molecular weights. The model predictions are consistent with this, and also with what is reported in the literature for other systems (for example, Morgan [23] for polyamide and Wolinski and Wronski [52] for polyarylate), as observed by Dhumal and Suresh [1]. In view of this, the observed trends in the present case are intriguing and bear further investigation. Further experiments were therefore carried out to get more data on the effect of the synthesis parameters R and n_L/V_d on molecular weight.

Fig. 20(a–c) shows the effect of n_L/V_d on M_W and polydispersity at different values of R. The model predictions are shown by lines. The cases shown in Fig. 20(a–c) corresponds respectively to HMDA being in excess ($R < 1$), stoichiometric equivalence ($R = 1$) and HMDI being in excess ($R > 1$). While model predictions show a monotonic behavior for both M_W and polydispersity in all cases, experimental trends are different for different cases. Thus, the results seem on the whole to be insensitive to n_L/V_d for $R < 1$, show an optimum at about $n_L/V_d = 0.9$ kmol/m^3 for $R = 1$, and show an increasing trend with n_L/V_d for $R > 1$. The trend with R seems to depend on monomer availability in the reaction zone, and correlates roughly with the end-of-run pH of the continuous phase, which decides the diamine availability towards the end. Below $R = 1$, the diamine availability remains high with pH around 11 (above the second dissociation constant of HMDA, $pKa_2 = 10.93$). At $R = 1$, even though the pH falls below the pKa_1 (first dissociation constant of HMDA = 9.83), diisocyanate availability also decreases

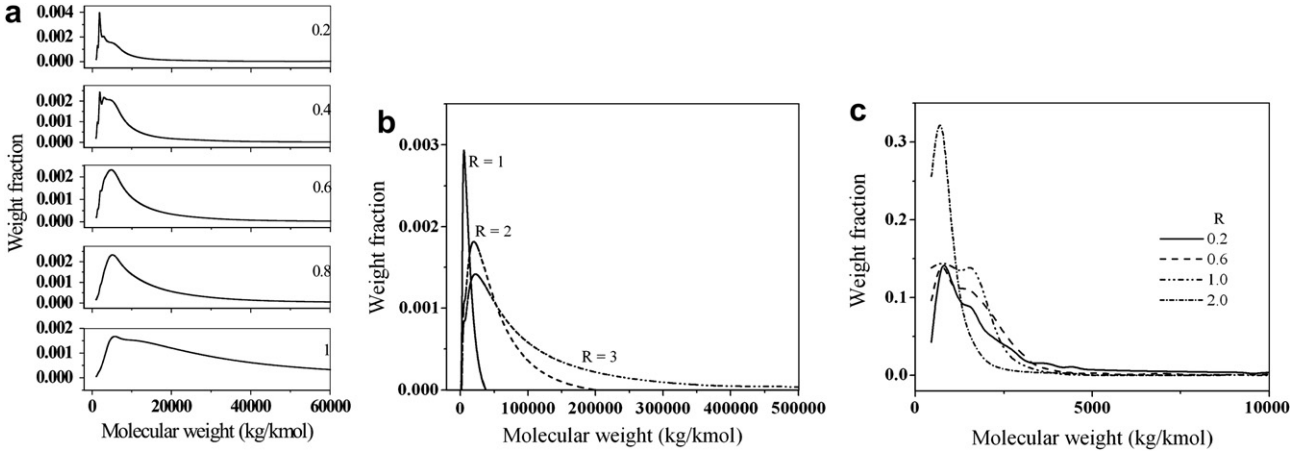

Fig. 18. Effect of R on MWD ($n_L/V_d = 0.545$ kmol/m^3): (a) $R \leq 1$ (b) $R \geq 1$ and (c) model predictions.

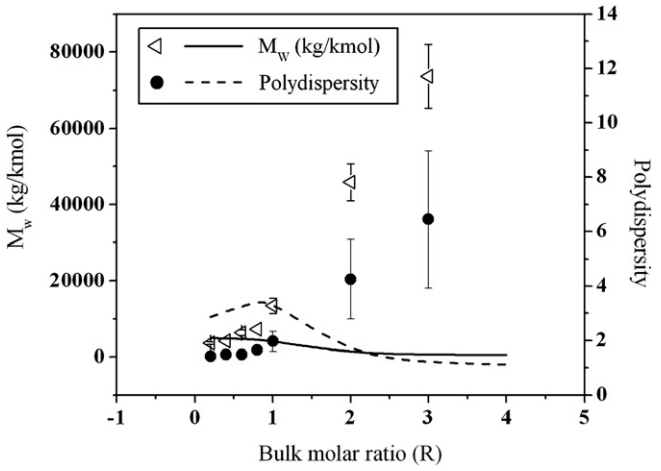

Fig. 19. Molecular weight and polydispersity variation with R ($n_L/V_d = 0.545$ kmol/m^3).

at the same time. For $R = 2$ the system pH falls to neutral indicating complete exhaustion of HMDA. In other words, experimental trends indicate that excess diamine keeps the molecular weight (and polydispersity) low while excess diisocyanate leads to a high molecular weight.

The above observations bring up the possibility that the molecular weights are being enhanced by some reactions not accounted in the model, and involving HMDI. FTIR was used to investigate this possibility. Fig. 21 compares the FTIR spectra of polyureas formed at different R in microencapsulation experiments. These show the appearance of stretching vibrations around 2705 cm^{-1}, which is characteristic of tertiary amino group [53]. This peak is almost absent below $R = 1$, and starts appearing just around $R = 1$, intensifying at higher values of R. It thus appears that the unreacted diisocyanate has some reactivity towards the secondary amine group of the urea linkage in polyurea (see Fig. 21) i.e. –NH – CO – NH– [54], and enters into reactions which ultimately lead to a degree of cross linking, thereby drastically increasing the molecular weight whenever excess diisocyanate is present. Clearly, such a reaction would become important only after the HMDA is exhausted, as the reactivity of the isocyanate group towards the primary amine group would be far greater. Molecular weights measured at intermediate conversion would not therefore show the effect of this reaction (and nor would any other aspect of the reaction, including kinetics). A certain amount of variability in the effect of this reaction should be expected even in the end-of-run molecular weights, since the extent of this reaction would depend on the time available between HMDA exhaustion and the filtering, crushing and washing of the microcapsules. This explains the large error bars seen in the molecular weight and polydispersity data for large R, in Fig. 21. Some of these samples were also difficult to dissolve in HFIP because of the high M_W/crosslinked nature. It may also be noted that it is the microcapsular configuration which allows the second reaction, since the unreacted diisocyanate monomer remains encapsulated and in contact with the film, and is not easy to remove. In situations such as of membrane synthesis, it would not

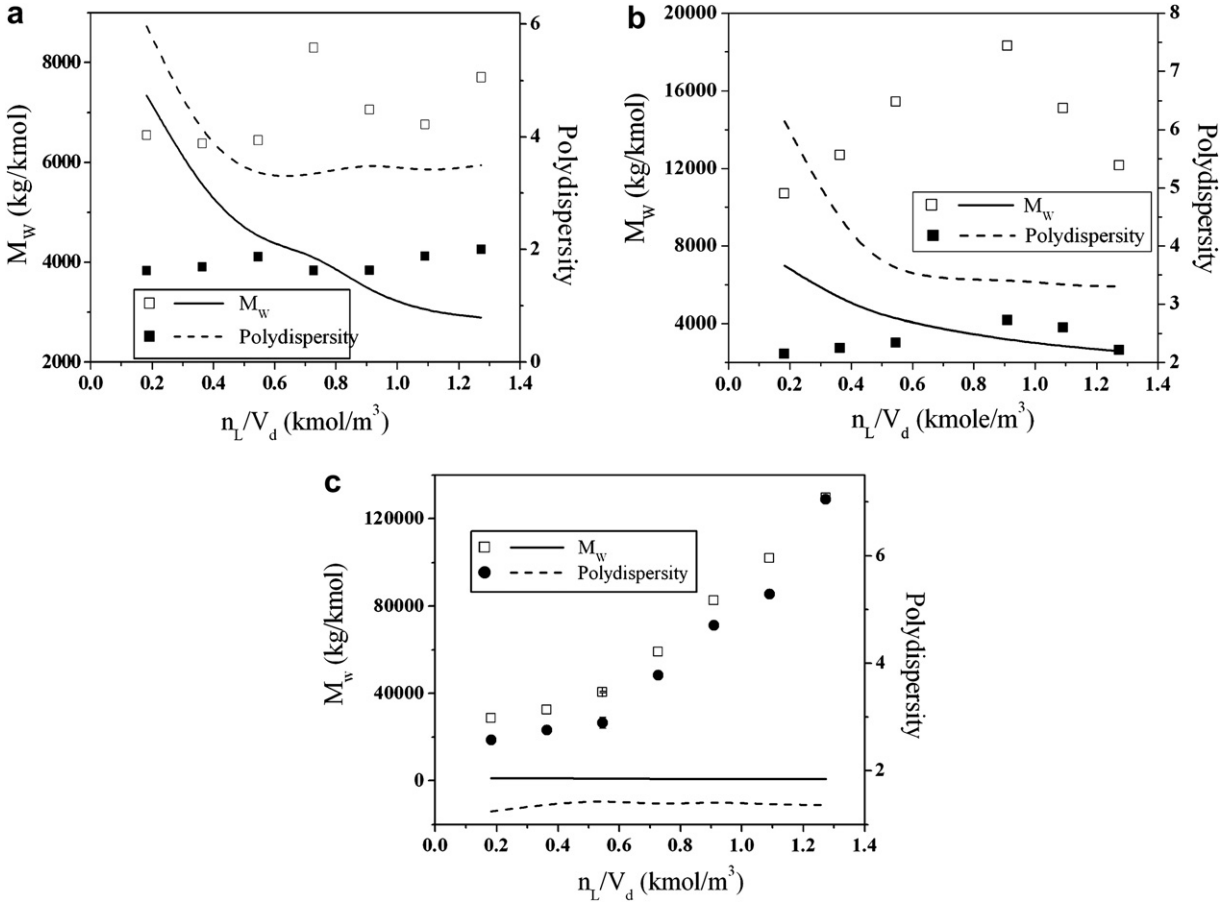

Fig. 20. Comparison of model predictions of molecular weight and polydispersity with experiments: (a) $R = 0.6$, (b) $R = 1$ and (c) $R = 2$.

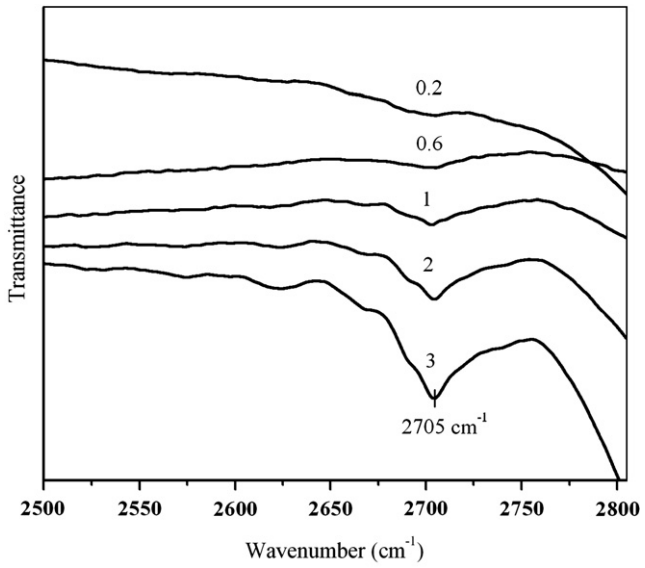

Fig. 21. FTIR spectra of polyurea microcapsule samples at different *R*.

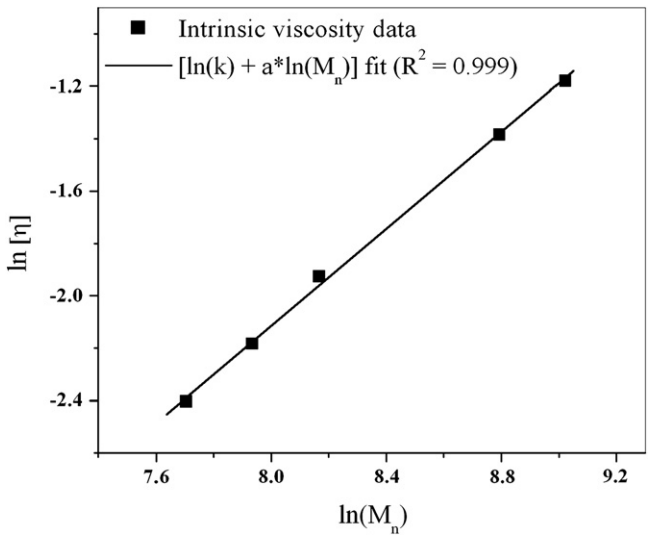

Fig. 23. Mark–Houwink (M–H) plot for polyurea (M–H parameters: $k = 7.46 \times 10^{-5}$, $a = 0.92$).

have any serious consequences. Even in microencapsulation, any commercial recipe would be such as to lead to total exhaustion of the isocyanate ($R < 1$), and the model would not need any modification for such cases.

The reaction scheme shown in Fig. 22 is therefore suggested as the reason for the counter-intuitive trends observed in the dependence of molecular weight on *R*. It should be emphasized that such side reactions are less likely in other systems such as polyamide, since the reactivity of acid chlorides towards amines is in general smaller than of isocyanates. These systems would therefore behave qualitatively according to the model of Dhumal and Suresh [1].

3.2.9. Mark–Houwink parameters for hexamethylene polyurea

The Mark–Houwink equation gives the relationship between intrinsic viscosity ($[\eta]$) and polymer molecular weight. In order to determine the parameters in this equation for polyurea, intrinsic viscosities were determined for some of the samples with 98% H_2SO_4 as the solvent as described earlier. Because of the problem of the secondary reaction mentioned earlier, polymers with large values of *R* such as 3, 4, etc. were excluded from this study. The average molecular weights from GPC analysis and the intrinsic viscosity determined by using Kraemers equation [43] have been used to prepare the plot shown in Fig. 23, in order to determine the M–H parameters for hexamethylene polyurea. From a search through literature compilations, it appears that this is the first time these parameters have been determined for this polymer. The estimated value of $a = 0.92$ is consistent with the polymer chains being semi-flexible ($0.8 < a < 2$) [55].

3.2.10. Solvent effect on polymer properties

The solvent plays a crucial role in polymer solution thermodynamics [44], since the binodal and spinodal envelopes ultimately control the polymer properties as observed by Dhumal and Suresh [1]. The solvent effect on kinetics, observed previously, determines the rate of formation and growth of polymer in a given reaction mixture, while the solubility limits decides the time spent during growth by any particular oligomeric species for a given rate of precipitation. In short, the reaction kinetics in combination with polymer thermodynamics determines the growth and precipitation rate of a particular oligomeric species. Table 3 shows the values of experimental molecular weights and crystallinity in different solvents under otherwise identical conditions of synthesis. The last column of the table compares the solvents in terms of the width of the metastable region, calculated from the Flory–Huggins theory as explained in Dhumal and Suresh [1]. The solvent effect can be analyzed from the relative magnitudes of the width of the metastable region and the chain growth rate constants. The broader the metastable region, the greater the opportunity for phase separation by nucleation and growth, and hence, the higher the crystallinity expected. On the other hand, the higher the rate constant, the faster the approach to spinodal decomposition and hence, the smaller the crystallinity expected. The metastable region is wider for toluene than for cyclohexane, but the rate constant is lower. These factors thus seem to balance out, with the result that the crystallinity is almost unaffected. The lower rate constant is seen to result in a growth of polymer chains as long as they remain in solution, with the result that the molecular weights are higher in toluene. Since the above considerations are built into the model formulation [1], the model is able to correctly predict these trends. Quantitative comparisons are however not possible since estimates of nucleation rate constant are not available for all solvents.

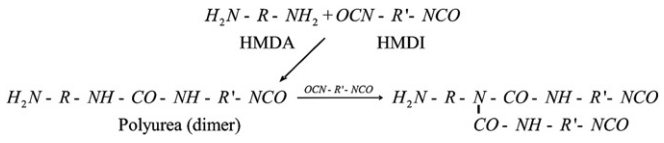

Fig. 22. Reaction of HMDI with the secondary amino group present in polyurea.

Table 3
Solvent effect on polymer properties.

Solvent	M_n (kg/kmol)	M_w (kg/kmol)	Polydispersity	Crystallinity	Metastable region width for 10 *B*
Cyclohexane	7095	11,407	1.608	0.375	8.09×10^{-3}
p-Xylene	9986	17,384	1.74	0.383	1.125×10^{-2}
Toluene	10,100	18,505	1.832	0.380	1.212×10^{-2}

4. Conclusions

A wide-ranging experimental study has been reported on the synthesis of poly(hexamethyleneurea), in microcapsule and flat-film geometries. The planning of the experimental studies has been with the objective of gaining an understanding of the underlying mechanisms. Thus a protocol was established for the characterization studies that eliminate the possibility of the sample characteristics being changed during sample preparation. Morphological studies show the film to be anisotropic, an aspect also confirmed by contact angle studies on the two surfaces of the film. Morphological studies, together with the observed effects of solvent-side variables, indicate the reaction to be on the organic side of the interface. Interfacial tension studies confirm that, in the presence of a surface active species, the role of the interface itself as a reaction locale is insignificant. The recent model of Dhumal and Suresh [1] has been used as a basis to interpret and understand the experimental findings. Using conditions under which kinetic control prevails, the reaction rate constants for the diamine–diisocyanate reaction in different solvents have been determined. The polarity of the solvent seems to be an important influence in determining these rate constants, which have been found to correlate with the dielectric constant of the solvent.

An array of techniques has been used to study the properties of film crystallinity, molecular weight and its distribution, and how they are influenced by the preparation conditions. In this heterogeneous system, phase separation mechanisms clearly play an important role in determining the properties of the polymer film that forms. In order to understand this, time course studies have been conducted on the development of film crystallinity and molecular weight. The crystallinity–conversion data have been used to estimate the nucleation rate constant that occurs in the model of Dhumal and Suresh [1] and controls all aspects of phase separation. The model has been shown to predict the observed trends on property development qualitatively.

The effect of preparation parameters on film properties has been studied. In most cases, the model is successful in predicting the observed trends qualitatively. Where there are discrepancies, diagnostic studies have been carried out to determine the causes. Thus, it appears that the consumption of diamine in the film as it diffuses towards the reaction zone has to be incorporated in the model formulation in order to achieve quantitative predictions. The molecular weight distributions seem to get modified because of the presence of a secondary reaction in cases of large R, towards the end of the experiment. Because of this, the observed trends, particularly of the molecular weight with R, are counter-intuitive and also at variance with literature findings on such systems. While this suggests that care is needed in choosing the data to be used in the testing of models, the side reaction identified affords a possibility of achieving a degree of cross linking and hence, an additional way to modify film properties.

The data collected in this work have been used to estimate the Mark–Houwink parameters for poly(hexamethyleneurea) for the first time.

The molecular weight (or more appropriately, the average chain length) is also important in determining the ease of crystallization and hence the degree of crystallinity achieved, under the constraints imposed by the other parameters of the system. This has been shown by DSC studies on a series of samples, which show a significant increase in the crystallization temperature with the molecular weight of the polyurea.

Overall, the results presented in this work provide useful insights into the mechanisms of property development in interfacial polyureas, and help in understanding the process better. They also provide directions for further modeling efforts in this area.

References

[1] Dhumal SS, Suresh AK. Polymer 2009;50(24):5851–64.
[2] LeGrand DG, Bendler JT. Handbook of polycarbonate science and technology. New York: Marcel Dekker; 2000.
[3] Chanda M, Roy SK. Plastic technology handbook. 4th ed. Florida: CRC Press; 2006.
[4] Chang TMS. Science 1964;146(3643):524–5.
[5] Khilar K. A State-of-the-art report on encapsulation. Bombay: I.I.T.; 1987.
[6] Green KD, Gill IS, Khan JA, Vulfson EN. Biotechnology and Bioengineering 1996;49(5):535–43.
[7] Yadav SK, Khilar KC, Suresh AK. Journal of Membrane Science 1997;125(2):213–8.
[8] Torini L, Argillier JF, Zydowicz N. Macromolecules 2005;38(8):3225–36.
[9] Cadotte JE. US Patent 4,039,440; August 2, 1977
[10] Desai NV, Rangarajan R, Rao AV, Garg DK, Ankleshwaria BV, Mehta MH. Journal of Membrane Science 1992;71(3):201–10.
[11] Peterson RJ. Journal of Membrane Science 1993;83(1):81–150.
[12] Rao AP, Desai NV, Rangarajan R. Journal of Membrane Science 1997;124(2):263–72.
[13] Jeong BH, Hoek EMV, Yan Y, Subramani A, Huang X, Hurwitz G, et al. Journal of Membrane Science 2007;294(1–2):1–7.
[14] Buch PR, Jagan Mohan D, Reddy AVR. Journal of Membrane Science 2008;309(1–2):36–44.
[15] Ghosh AK, Jeong BH, Huang X, Hoek EMV. Journal of Membrane Science 2008;311(1–2):34–45.
[16] Moniruzzaman M, Chattopadhyay J, Billups WE, Winey KI. Nano Letters 2007;7(5):1178–85.
[17] Tarameshlou M, Jafari SH, Khonakdar HA, Farmahini-Farahani M, Ahmadian S. Polymer Composites 2007;28(6):733–8.
[18] Cranmer JH, Tesoro GC, Uhlmann DR. Industrial and Engineering Chemistry Product Research and Development 1982;21(2):185–90.
[19] Salehi-Mobarakeh H, Ait-Kadi A, Brisson J. Polymer Engineering and Science 1996;36(6):778–85.
[20] Hisamoto H, Shimizu Y, Uchiyama K, Tokeshi M, Kikutani Y, Hibara A, et al. Analytical Chemistry 2003;75(2):350–4.
[21] Jong J, Lammertink RG, Wessling M. Lab on a Chip 2006;6(9):1125–39.
[22] Parrish CF. US Patent 7285306; October 23, 2007.
[23] Morgan PW. Condensation polymers: by interfacial and solution methods. New York: Wiley; 1965.
[24] Millich F, Carraher Jr CE. In: Fundamentals. Interfacial synthesis, vol. I. New York: Marcel Dekker; 1977.
[25] Millich F, Carraher Jr CE. In: Polymer applications and technology. Interfacial synthesis, vol. II. New York: Marcel Dekker; 1977.
[26] Carraher Jr CE, Preston J. In: Recent advances. Interfacial synthesis, vol. III. New York: Marcel Dekker; 1982.
[27] Korshak VV, Vasnev VA. Interfacial and dispersion polymerization. In: Allen G, Bevington JC, Rooth C, Price C, editors. Comprehensive polymer science–the synthesis, characterization, reactions and applications of polymers, vol. 5. Oxford: Pergamon Press; 1989. p. 167–96.
[28] Mathiowitz E, Cohen MD. Journal of Membrane Science 1989;40:1–26.
[29] Mathiowitz E, Cohen MD. Journal of Membrane Science 1989;40:27–42.
[30] Mathiowitz E, Cohen MD. Journal of Membrane Science 1989;40:43–54.
[31] Mathiowitz E, Cohen MD. Journal of Membrane Science 1989;40:55–65.
[32] Mathiowitz E, Cohen MD. Journal of Membrane Science 1989;40:67–86.
[33] Berezkin AV, Khokhlov AR. Journal of Polymer Science, Part B: Polymer Physics 2006;44:2698–724.
[34] Janssen L, Nijenhuis K. Journal of Membrane Science 1992;65(1–2):59–68.
[35] Bouchemal K, Couenne F, Briancon S, Fessi H, Tayakout M. AIChE Journal 2006;52(6):2161–70.
[36] Bradbury JH, Crawford PJ, Hambly AN. Transactions of the Faraday Society 1968;64:1337–47.
[37] Tsai HB, Jeng JT, Tsai RS. Journal of Applied Polymer Science 1990;39:471–6.
[38] Yadav SK, Khilar KC, Suresh AK. AIChE Journal 1996;42(9):2616–26.
[39] Wang CY, Wang DC, Chiu WY, Chen LW. Die Angewandte Makromolekulare Chemie 1997;248:123–37.
[40] Wagh SJ, Dhumal SS, Suresh AK. Journal of Membrane Science 2009;328(1–2):246–56.
[41] Goyal N, Suresh AK. In: Proceedings in international conference on advances in chemical engineering. IIT Madras, Chennai, India; 1996.
[42] Wamser CC, Gilbert MI. Langmuir 1992;8(6):1608–14.
[43] Kinsinger JB. Viscometry. In: Mark H, Gaylord NG, Bikales N, editors. Encyclopedia of polymer science and technology, vol. 14. New York: Wiley Interscience; 1971.
[44] Dhumal SS, Wagh SJ, Suresh AK. Journal of Membrane Science 2008;325(2):758–71.
[45] MacRitchie F. Transactions of the Faraday Society 1969;65:2503–7.
[46] Ryan AJ, Stanford JL. Polyureas. In: Eastmond GC, Ledwith A, Russo S, Sigwalt P, editors. Comprehensive polymer science, vol. V. Oxford: Pergamon Press; 1989. p. 427–54.
[47] Berode M, Test B, Savolainen H. Toxicology Letters 1991;56(1–2):173–8.
[48] Cadotte JE, King RS, Majerle RJ, Peterson RJ. Interfacial synthesis in preparation of reverse osmosis membranes. In: Carraher Jr CE, Preston J, editors. Recent advances. Interfacial synthesis, vol. III. New York: Marcel Dekker; 1982. p. 47–75.
[49] Chern YT, Wu BS. Journal of Applied Polymer Science 1996;61(11):1853–63.

[50] Nakache E, Dupeyrat M, Vignes-Adler M. Faraday Discussion of the Chemical Society 1984;77:189–96.
[51] Yadav SK, Ron N, Chandrasekharam D, Khilar KC, Suresh AK. Journal of Macromolecular Science – Physics 1996;35(5):807–27.
[52] Wolinski J, Wronski S. Chemical Engineering and Processing: Process Intensification 2009;48(5):1061–71.
[53] Khan MA, Kumar S, Jaychandran J, Vartak SV, Bhartiya A, Sinha S. Chromatographia 2005;61(11–12):599–607.
[54] Lapprand A, Boisson F, Delolme F, Méchin F, Pascault J-P. Polymer Degradation and Stability 2005;90(2):363–73.
[55] Brandrup J, Immergut EH. Polymer handbook. 3rd ed. New York: Wiley; 1989.